

Analysis of Four-Dimensional Cardiac Data Sets Using Skeleton-Based Segmentation

André Neubauer
VRVis Research Center
Donaucitystraße 1
1220 Vienna, Austria
neubauer@vrvis.at

Rainer Wegenkittl
VRVis Research Center
Donaucitystraße 1
1220 Vienna, Austria
wegenkittl@vrvis.at

ABSTRACT

Computer-aided analysis of four-dimensional tomography data has become an important tool in modern cardiology. In order to examine the capability and health of a patient's cardiac system, scans are taken at a number of time points evenly distributed over one cardiac cycle. A key task for understanding the dynamics involved within a recorded cardiac cycle is to segment the acquired data to identify objects of interest in each volume of the sequence. This paper presents an algorithm to segment the heart muscle and the left ventricle from a sequence of cardiac CT images using only a minimum of user interaction. Furthermore, the paper introduces methods to process the segmentation result for extraction of important properties of the cardiac cycle, which are helpful for diagnosis.

Keywords

Heart Function Analysis, Myocardium, Left Ventricle, Segmentation

1 INTRODUCTION

Acquisition and analysis of four-dimensional tomography data has grown to become an important tool for computer-aided analysis of human cardiac activity. Scans are usually taken at about 10 to 20 time points evenly distributed over one cardiac cycle. The acquired data can then be analyzed and evaluated to give an overall picture of the heart's capability and health. A key task for understanding the dynamics involved within a recorded cardiac cycle is to segment each acquired data volume to identify objects of interest. One interesting part of the heart is the heart muscle (myocardium). It encloses the left ventricle (LV) of the heart and, by contracting and expanding, makes blood diffuse out of the ventricle into the entire body. Properties of the myocardium and the LV as a function of both time and space reflect the state of the patient's cardiac system very

well. Crucial properties include the change of myocardial wall thickness over time as well as the volume of the blood perfused during one cardiac cycle.

Preferred data acquisition modalities include Magnetic Resonance Imaging (MRI) and Computer Tomography (CT). Many authors concentrate on data acquired from MRI, only comparably few publications consider CT data. There are two main reasons for this fact: Firstly, during an MRI examination, the body is not exposed to heavy radiation, as during a CT examination. MRI is therefore the healthier scanning method. A second reason is the higher level of flexibility. MRI is, for instance, capable of projecting a magnetic tag pattern onto body tissue (MRI-SPAMM). These tags move along with the tissue and therefore can help tracking the motion of the myocardial walls, for example.

However, the usage of a CT also bears advantages. Due to special fast techniques, like Electronic Beam CT (EBCT) or the more recently developed multi-slice CT, CT scans can be generated faster than MRI scans. Therefore four-dimensional CT images, other than MRI ones, can usually be well resolved in all three spatial dimensions *and* the time dimension. Another advantage is that in an image acquired from a CT, the intensity contrast between the myocardium and surrounding tissue is usually more recognizable

Permission to make digital or hard copies of all or part of this work for personal or classroom use is granted without fee provided that copies are not made or distributed for profit or commercial advantage and that copies bear this notice and the full citation on the first page. To copy otherwise, or republish, to post on servers or to redistribute to lists, requires prior specific permission and/or a fee.

Journal of WSCG, Vol.11, No.1., ISSN 1213-6972
WSCG'2003, February 3-7, 2003, Plzen, Czech Republic.
Copyright UNION Agency – Science Press

than in a corresponding MRI image, which makes segmentation easier and more accurate.

This paper deals with segmentation of the myocardium and the LV from a four-dimensional CT data set and explains, how the two important properties mentioned above can easily be computed. The algorithms used are based on Skeleton-Based Myocardium Segmentation, a previously published algorithm [Neu03a] for segmenting the myocardium in a 3D data set, which will be roughly outlined in section 3. Section 4 describes the extension of the segmentation algorithm to the fourth dimension. Section 5 explains the calculation of myocardial wall thickness, section 6 deals with segmentation of the LV and the calculation of blood perfusion volume.

2 SEGMENTATION TECHNIQUES

Much scientific work has been done in the field of analysis of four-dimensional data sets of cardiac cycles. This section presents techniques proposed for segmentation of the myocardium and the LV and evaluates their capabilities of segmenting four-dimensional cardiac data sets.

A very widely used technique is the *deformable model* method which exploits constraints derived from the image data together with a-priori knowledge about the location, size and shape of the segmented objects [Kas87a, McI96a, Rue97a]. A boundary is initialized close to the expected final result. Then forces are applied to align the boundary with real object contours. Jones and Metaxas [Jon97a] use pixel affinity (a measure of probability that two neighboring pixels belong to the same object) and balloon forces [Coh91a] to initialize a deformable model. The LV boundary is initialized in the middle of the LV and iteratively enlarged into all directions until pixels of low affinity are reached. The problem is that noise and papillary muscles (small muscles inside the LV) might lead to bad initialization. Also, this technique only segments the LV and not the myocardium. An advantage is that it can easily be extended to the fourth dimension. Chakraborty and Duncan introduced an approach to refine an initialized boundary by methods based on game theory [Cha95a]. Two modules, one representing region-based segmentation, the other representing boundary-based segmentation, work in a coordinated fashion towards a common goal, the segmentation of an object of interest. Results, however, are only reported for 2D segmentation of the LV.

Some authors propose to segment the LV and in each slice initialize the outer boundary of the myocardium (the epicardium) as a shape similar to the boundary of the LV (the endocardium) and then refine this estimation to better fit the data [San95a]. Usually

these techniques miss a significant part of the myocardium, since not every slice that intersects the myocardium also intersects the LV.

Urschler et al. used the Live-Wire [Mor92a] technique for segmentation of the LV [Urs02a]. Their method works well distinguishing the LV from the left chamber of the heart, which is a tough problem as outlined in section 6. This, however, is achieved at the cost of a big amount of interaction needed for segmenting each time-step. They do not report, how the technique performs for myocardium segmentation.

Drobics et al. use self-organizing maps (SOM) to segment the myocardium in a three-dimensional data set [Dro02a]. By using the resulting (trained) SOM as an initialization for segmenting neighboring volumes in a 4D data set, the result can be propagated well in time dimension, enabling 4D segmentation. The authors state, however, that current segmentation results still require some manual post-processing.

Spreeuwers and Breeuwer presented a method [Spr01a] that automatically detects the myocardium boundaries in cardio perfusion scans, by exploiting changes in the relation of contrast agent concentration between the myocardium and surrounding tissue over time.

As already pointed out, many publications deal with techniques based on MRI-SPAMM and propose methods of utilizing MRI tagging for delineation of the motion of the LV and the heart muscle [Den94a, Zer88a].

3 SKELETON-BASED MYOCARDIUM SEGMENTATION

This section gives an overview of the previously published technique for segmenting the myocardium in three-dimensional CT data sets of human hearts [Neu03a]. This segmentation algorithm consists of three major parts: manual marking, skeleton propagation and segmentation refinement. They are explained in more detail in the following paragraphs:

3.1 Manual marking

The user selects a slice of the 3D data set and marks the cross-section of the myocardium in this slice by setting a number of representative *skeleton knots*. This step is the only part of the algorithm which takes user interaction. The poly-line made up by the skeleton knots forms an approximated skeleton of the cross-section of the myocardium.

3.2 Skeleton propagation

After a 2D skeleton has been placed onto one slice by the user, it is automatically propagated to the other slices of the 3D data set. For each slice, first the

skeleton is copied from a neighboring slice, and then it is adjusted to provide a better representation of the myocardial cross-section. Adjustment consists of the following four steps: data analysis, boundary detection, centering and maintenance.

3.2.1 Data Analysis

First, the data underneath the skeleton is analyzed. The average values and standard deviations both for data values and gradients are calculated by taking evenly spaced samples all over the 2D skeleton.

3.2.2 Boundary Detection

The statistical properties calculated in the first step are used for estimating boundary points. For each skeleton knot, a vector v , which is parallel to the current slice and close to normal to the skeleton, is calculated. Now, starting from the skeleton knot, data samples are taken in direction of v . The distance between samples is equal to the sampling distance used in the data analysis step. As soon as data values and/or gradients are encountered, which diverge significantly from the calculated average values (with respect to the standard deviations) the algorithm assumes that a boundary point has been found. In order to increase stability, this process is repeated n times for each skeleton knot, using n slightly different sampling directions. The resulting n points are sorted by distance to the skeleton knot. Those m (in the current implementation, n is 11 and m is 4) points with smallest distance are discarded as well as those m points with largest distance. The final boundary point is then calculated by averaging the coordinates of the remaining $n-2m$ points. For each skeleton knot, another boundary point is then searched in the opposite direction ($-v$).

3.2.3 Centering

The result of the second step is a set of $2p$ boundary points, with p being the number of skeleton knots. In the third step, each skeleton knot is moved to the exact center between two opposite boundary points.

3.2.4 Maintenance

In order to ensure robust propagation of the 2D skeleton, certain properties of the skeleton must be watched and controlled. The skeleton may have to be extended or shortened to provide a reasonable representation of the cross-section of the myocardium. Skeleton knots may have to be added, removed or reordered. Also, possible reasons for instability, like geometry changes of the myocardial cross-section, have to be detected and dealt with.

3.2.5 Segmentation Refinement

After the first two steps of the algorithm, the collection of all 2D skeletons can be seen as a skeleton of the entire myocardium (see Figure 1, left image). Now segmentation is done by finding all

voxels of the data set, that belong to the myocardium. For this, a cost value is calculated for each voxel, denoting the cost of the cheapest path from the voxel to a voxel that is part of the skeleton. The cost of a path is determined by its length and the data values that it passes through.

Segmentation can now be finished by grouping all voxels with a cost value smaller than a certain threshold to the final segmented object. A suitable threshold can easily be found by detecting distinct gradients in the cost volume and choosing the threshold such that these distinct gradients represent parts of the object boundary. A segmented myocardium is depicted in Figure 1. The visualization was done by iso-surfacing in the volume consisting of cost values.

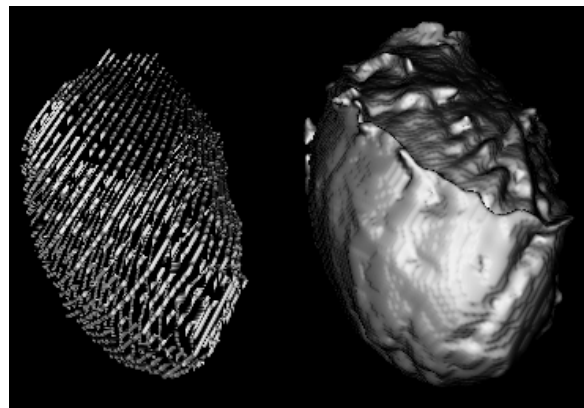


Figure 1. a segmented heart muscle (right) and its 3D skeleton (left)

4 EXTENSION TO 4D

The method described so far can easily be extended to process 4D data sets, i.e., data sets consisting of a number of volumes, each representing one time point in a cardiac cycle. The simplest way to do this is, of course, to apply the proposed 3D segmentation technique to each volume. This, however, induces unnecessarily much need for interaction, since an initial 2D skeleton must be manually placed to each volume. Instead, the result of segmenting the volume representing time point t can be used to initialize segmentation of the volumes representing time points $t-1$ and $t+1$. The idea is to segment one volume using the 3D method and fully automatically propagate the result to the other ones. Of course, only the skeleton has to be propagated. The final segmentation result can then be obtained for each volume independently by applying a cost function, as outlined in section 3.2.5.

A 4D data set can be seen as a matrix of slices – one dimension of the matrix being a spatial dimension and the other being the time dimension. Some of

those slices contain cross-sections of the myocardium and are therefore of special interest. The 3D algorithm propagates a skeleton representing a cross-section of the myocardium from slice to slice within one 3D data set, i.e., in the spatial dimension. Now the need emerges to propagate skeletons in time dimension. This is more difficult for the following reason: The resolution in time dimension is usually substantially lower than in each of the spatial dimensions, and thus changes between neighboring slices can be more significant. However, two cross-sections of the myocardium, which are on neighboring slices in time dimension, usually do overlap. The following sections show, how a slight overlap can be used to propagate a 2D skeleton from one slice to another in time dimension and explain two ways of propagating a complete segmentation result to another volume.

4.1 Propagation of a Skeleton in Time Dimension

This section describes the process of fitting a 2D skeleton from one slice (the source slice) to another (the destination slice), with source and destination slices being neighbors in time dimension. The volume containing the source slice has already been segmented, E_i denotes the average data value and S_i denotes the standard deviation of voxels assigned to the myocardium in the source volume.

The algorithm, illustrated in Figure 2, roughly consists of three parts: First, the region, where the two cross-sections of the myocardium overlap, is identified. Then the skeleton is transferred to this region of overlap. Finally, the skeleton is centered on the cross-section of the myocardium on the destination slice.

The overlap region is found by assigning each voxel in the destination slice a value expressing the probability that the voxel is part of the overlap region. These probability values are initialized to 1 for all those voxels whose direct counterparts in the source slice were found to be part of the myocardium and to 0 for all others. Then the probability value of each voxel is multiplied by a coefficient c :

$$e^{-\frac{(v-E_i)/S_i}{2}} \quad (\text{Equation 1})$$

with v being the data value at the voxel. Equation 1 is a slight adaptation of a formula published by Jones et al. [Jon97a]. The resulting matrix of probability values is blurred a few times. This is done to generate a smooth relief with local maxima near the center line of the overlap. In the next step, the 2D skeleton is copied from the source to the destination slice and adapted by moving its knots to local maxima in the

probability matrix. The center image in Figure 2 shows an iso-contour in the probability matrix and the adapted skeleton. The last step, the centering of the skeleton (see Figure 2, right image) on the cross-section of the myocardium in the destination slice, is done like in the 3D algorithm (see sections 3.2.2 and 3.2.3), with only one exception: For reasons of stability, the skeleton is not allowed to move out of the overlap region. This prevents chaotic behavior in case, the destination volume is of poor quality (see Figure 3, right image).

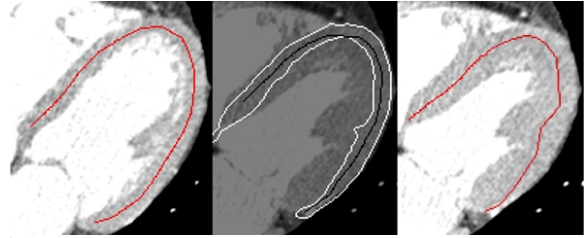


Figure 2. propagation of a 2D skeleton, left: source slice with 2D skeleton, right: destination slice with 2D skeleton, middle: overlap region with 2D skeleton

4.2 Propagation of a Segmentation Result in Time Dimension

There are two ways of propagating a complete 3D segmentation result to a neighboring volume in time dimension. The quality of the destination volume decides, which of them should rather be used. It is possible that a sequence of CT images contains one or more volumes of poor quality (see Figure 3, right image). For those volumes, segmentation is difficult, as the average data value for voxels inside the myocardium significantly differs from other volumes in the sequence and, which is worse, the variance is much higher. Still, a reasonable segmentation result is required. The best way to achieve this is to prevent the skeleton in the destination volume from deviating too much from the skeleton in the source volume. This can be done by propagating 2D skeletons to the destination volume solely in time dimension (see previous section). On the first glance, the following fact could be considered troublesome: Since the myocardium contracts and expands during the cardiac cycle, the number of slices it intersects usually differs among the volumes of a sequence. The obvious consequence is that if a slice intersects the myocardium near the top or the bottom of the heart muscle, this does not automatically imply that its two neighbors in time dimension also contain a cross-section of the heart muscle. Therefore, if the skeleton is only propagated in time dimension, not every slice intersecting the myocardium might be assigned a skeleton. However, experiments showed that this fact is not really a problem, because the skeleton usually

needs not reach every cross section of the myocardium. It is sufficient for the skeleton to roughly describe the shape of the myocardium in order to provide a sound basis for the cost function which determines the final result.

In higher quality volumes (see Figure 3, left image), a more intuitive strategy is to transfer only one 2D skeleton from the source volume to the destination volume and propagate the skeleton within the destination volume using the 3D algorithm.

After the skeleton has been propagated to a volume, segmentation is performed as explained in section 3.2.5.

Due to propagation from volume to volume and from slice to slice, an error happening in one slice can accumulate during further propagation. The propagation algorithm, however, proved to work robustly propagating along a distance of up to 10 time steps.

Segmenting a 4D data set currently takes about one minute per volume plus about 30 seconds for the user interaction part.

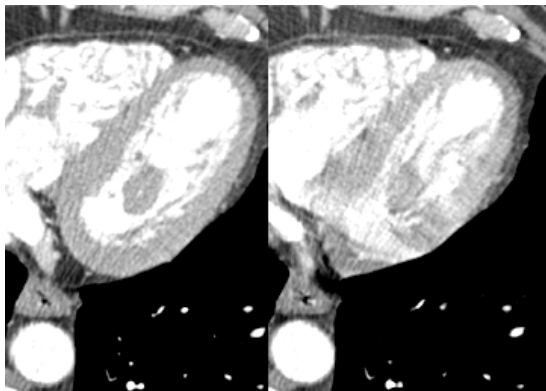


Figure 3. high quality (left) and low quality (right) scans

5 MYOCARDIAL WALL THICKNESS

Myocardial wall thickness as a function of time is an important parameter in the assessment of heart function. Calculation of myocardial wall thickness is first of all a matter of definition of the term ‘wall thickness’. One possible definition, which is also the one used in this paper, is that the thickness at a given point on the outside boundary of the heart muscle (the epicardium) is the minimal distance to the inside boundary (the endocardium) and vice versa. There are some ways of calculating the thickness for a given point:

Eusemann et al. [Eus01a] proposed to precompute a chamfer distance map that encodes for each voxel the distance to the LV and take the distance value as

myocardium thickness for voxels on the epicardium. The disadvantage of this algorithm is that thickness values must be kept in memory during the process of analysis. In a data set of usual size (e.g., about $512 \times 512 \times 300$ voxels), additional memory consumption will amount to more than 314 MB, if 4-byte floating-point values are used. Sometimes, therefore, it is a better decision to quickly extract the thickness for a given voxel on the boundary of the heart muscle on the fly, when needed (e.g., during rendering).

One possible algorithm is to grow a three-dimensional distance field from the point of interest until a point on the other part of the myocardial boundary is encountered. The drawback of this technique is that its cost grows cubically with wall thickness.

Experiments showed the applicability of the following algorithm: For a given point on one part of the myocardial boundary (epicardium or endocardium), the nearest point (the ideal counterpart) on the other part of the boundary is searched. The idea is to quickly find a counterpart that is close to ideal and start a local search procedure to find the ideal one. The result of the segmentation algorithm presented in section 3 is a data volume denoting for each voxel the cost of the cheapest path to the skeleton. The boundaries of the segmented object are found by extracting an iso-surface in this volume. Therefore, for each point on the object boundary, the surface normal can easily be found by calculating the image gradient vector. A ray is cast at the point, for which the thickness shall be computed, in opposite direction of the surface normal and (if the point is located on the epicardium) intersected with the endocardium. From the intersection point, a local search procedure is started: The algorithm keeps moving in direction of the most significant decrease of distance to the examined point until a minimum and thus the final counterpart is found. The thickness is then the distance between the point and its counterpart. The problem with this algorithm is that it can get stuck in local minima. The probability of finding the global minimum can be increased significantly by repeating the process a couple of times, with slightly different ray direction vectors. Figure 4 depicts the result of a wall thickness calculation: The left image shows a segmented myocardium, the right image shows the same myocardium with wall thickness mapped to light intensity.

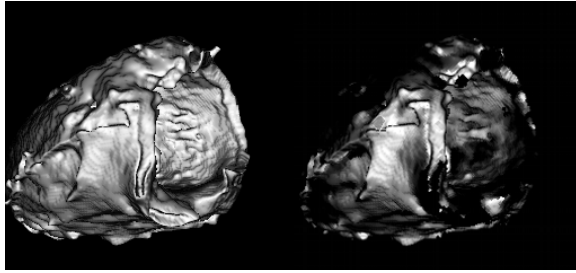


Figure 4. myocardial wall thickness

6 BLOOD PERFUSION VOLUME

Another important aspect of heart function is blood perfusion volume. The volume of the blood contained by the left ventricle strongly varies throughout the cardiac cycle. It is at its highest level, when the myocardium is expanded (the end of diastole) and at its lowest level when the myocardium is contracted (the end of systole). The difference is the volume of the blood that was perfused during the scanned cardiac cycle.

To calculate the blood perfusion volume, it is necessary to segment the left ventricle and calculate its volume in each 3D image of the sequence. The difference between the minimal and maximal volumes is the blood perfusion volume.

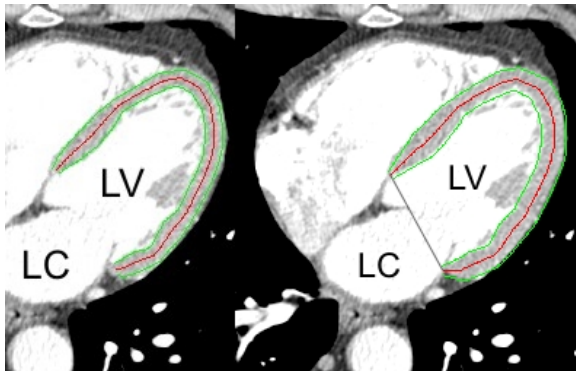


Figure 5. left ventricle (LV) and left chamber (LC), and the approximated boundary (right)

The boundary between left ventricle and left chamber of the heart is usually not captured well by tomography. Therefore it is hard to automatically distinguish these two parts of the heart (see Figure 5). Radiologists, however, find it sufficient to approximate the left ventricle as the space enclosed by the heart muscle. Thus segmentation of the myocardium can help segmenting the left ventricle in the following way: In each slice, the 2D skeleton is extended towards the two ends of the cross-section of the segmented heart muscle (see Figure 6). Then the imaginary line between the two ends of the skeleton is used as an approximated boundary between the left ventricle and the left chamber (see Figure 5, right

image). After that, each voxel located in the area enclosed by the skeleton and the approximated boundary between LV and LC is assigned to the LV if it does not represent a part of the myocardium.

In order to get a good approximation of left ventricular volume, it is important to exclude the papillary muscles (small muscles inside the ventricle) from the LV. This can be done by calculating a coefficient for each voxel of the LV indicating the probability that the voxel represents a part of a muscle. Since the voxels representing the papillary muscles are at a similar intensity level as those representing the heart muscle, equation 1 can be used to calculate these coefficients, with E_i being the average and S_i the standard deviation of the intensity values encountered in the myocardium. Then all those voxels whose coefficients are below a certain threshold are selected to represent the LV. Here, a suitable threshold is the low point of the first derivative of the function mapping to each coefficient the number of voxels with higher coefficients. The segmentation result for one slice is depicted in Figure 7. Here the pixels rendered lightly (except those which are part of the skeleton) were assigned to the LV. Figure 8 shows two renderings of the segmented complete LV. The visualization was done by iso-surfacing in the volume made up by the coefficients. At the open end of the ventricle, the slice-wise approximations of the LV boundary are well visible.

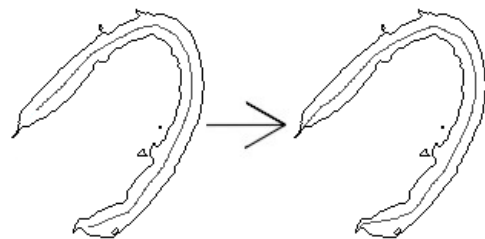


Figure 6. Extension of the skeleton

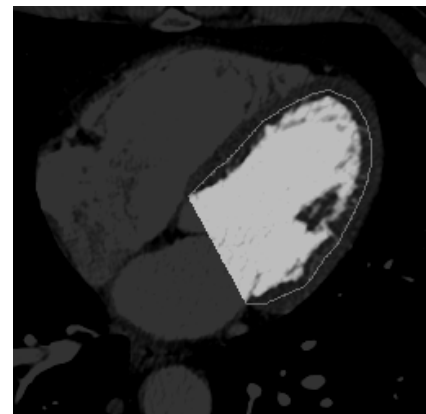


Figure 7. LV segmentation (2D)

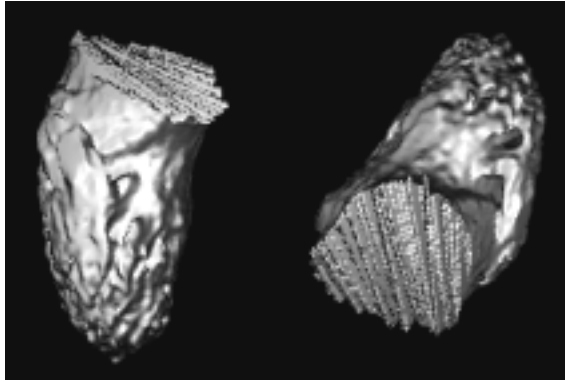


Figure 8. LV segmentation (3D)

7 RESULTS

The algorithms presented in this paper were tested on multi-slice CT data sets of human hearts to verify their applicability. Figure 9 shows a sequence of heart muscles obtained from segmenting one 4D data set. Figure 10 depicts a sequence of left ventricles from the end of systole to the end of diastole. Figure 11 shows a sequence of segmented cross-sections from the end of systole to the end of diastole.

8 CONCLUSION

This paper described, how Skeleton-Based Myocardium Segmentation can be used to aid the analysis of human heart function. A technique to segment four-dimensional CT data sets of the human heart was presented as well as techniques to process the segmentation result to assess important parameters of heart function. It was shown that Skeleton-Based Myocardium Segmentation provides good prerequisites for fully automatic extension to 4D, the calculation of myocardial wall thickness and the calculation of blood perfusion volume.

Although the proposed techniques proved to work well, there is still work in process to improve them as well as to find alternative approaches for sub tasks.

More illustrations and animations can be found on <http://stud3.tuwien.ac.at/~e9625734/seg>.

9 ACKNOWLEDGEMENTS

This work has been carried out as part of the basic research project 'Virtual Reality for Scientific Applications' at the VRVis Research Center (www.vrvis.at) in Vienna, Austria, which is funded by the Austrian governmental research project Kplus. Thanks to Tiani Medgraph AG (www.tiani.com) for providing useful implementation facilities.

10 REFERENCES

- [Cha95a] Chakraborty, A. and Duncan, J., S. Integration of Boundary Finding and Region-Based Segmentation Using Game Theory. In XIVth International Conference on Information Conf.proc. pp. 189-200, 1995
- [Coh91a] Cohen, L., D. On Active Contour Models and Balloons. CVGIP: Image Understanding 53(2). pp. 211-218, 1991
- [Den94a] Denney, T., S., Prince, J., L., Lopez, M., J., and McVeigh, E., R. Optimal Tag Pattern Validation Using Magnetic Resonance Imaging. First IEEE International Conference on Image Processing, Austin, TX. Conf.proc. pp. 881-885, November, 1994
- [Dro02a] Drobics, M., Hobelsberger, P., M., Wegenkittl, R. Analysis and Visualization of 4D Medical Images Using Self-Organizing Maps and Clustering. 26th Workshop of the Austrian Association for Pattern Recognition (AAPR), Graz, Austria, September 10-11, 2002
- [Eus01a] Eusemann, C., S. Mohlenkamp, E.L. Ritman, R.A. Robb: 3D Quantitative Visualization of Altered LV Wall Thickening Dynamics Caused by Coronary Microembolization. In SPIE Medical Imaging 2001: Physiology and Function From Multidimensional Images. Conf.proc. 4321:100-107, 2001
- [Jon97a] Jones, T.N., and Metaxas, D.N. Segmentation Using Deformable Models with Affinity-Based Localization. In CVRMed-MRCAS 1997 Conf.proc., pp.53-62, 1997.
- [Kas87a] Kass, M., Witkin, A., and Terzopoulos, D. Snakes: Activated Contour Models. In First International Conference on Computer Vision, London, UK, 1987
- [McI96a] McInerney, T., and Terzopoulos, D. Deformable models in Medical Image Analysis: A Survey. Medical Image Analysis 1(2), pp. 91-108, 1996.
- [Mor92a] Mortensen, E., N., Morse, B., S., Barrett, W., A., and Udupa, J., K. Adaptive Boundary Detection Using 'Live Wire' Two-Dimensional Dynamic Programming. In IEEE Proceedings of Computers in Cardiology (CIC '92), pp. 635-638, Durham, NC, Oct. 1992
- [Neu03a] Neubauer, A., and Wegenkittl, R. Skeleton-Based Myocardium Segmentation. In SPIE Visualization and Data Analysis 2003 Conf. proc., 2003 (to appear)
- [Rue97a] Rueckert, D. Geometrically Deformable Templates for Shape-Based Segmentation and Tracking in Cardiac MR Images. EMMCVPR 1997: pp. 83-98, 1997

[San95a] Sánchez-Ortiz, G., I., Burger, P. Vector Field Analysis of the Dynamics of the Heart using Velocity Encoded Cine MR Imaging. In 9th International Symposium on Computer Assisted Radiology, CAR'95 Conf.proc. pp 228-233, Berlin, June 1995

[Spr01a] Spreeuwers, L. and Breeuwer, M. Automatic Detection of the Myocardial Boundaries of the Right and Left Ventricle in MR Cardio Perfusion Scans. In *Proceedings of the SPIE Conference on Medical Imaging*, volume 4322, pp 1207-1217, San Diego, USA, Feb 2001.

[Urs02a] Urschler, M., Mayer, H., Bolter, R., Leberl, F. The Live-Wire Approach for the Segmentation of Left Ventricle Electron-Beam CT Images. 26th Workshop of the Austrian Association for Pattern Recognition (ÖAGM/AAPR), 2002

[Zer88a] Zerhouni, E., A., Parish, D., M., Rogers, W., J., Yangand, A., and Shapiro, E. P. Human Heart: Tagging with MRI Imaging – a Method for Non-Invasive Assessment of Myocardial Motion. *Radiology*, 169:59-63, 1988.

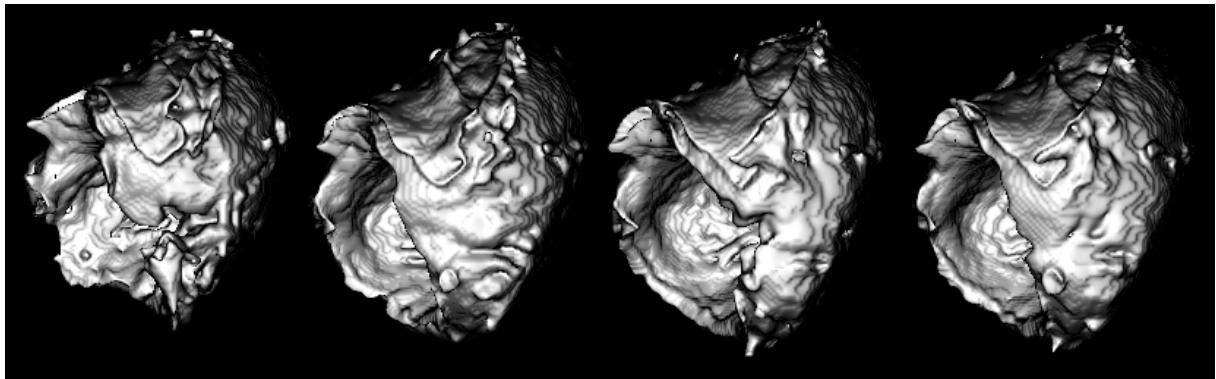


Figure 9. the heart muscle at different points in the cardiac cycle

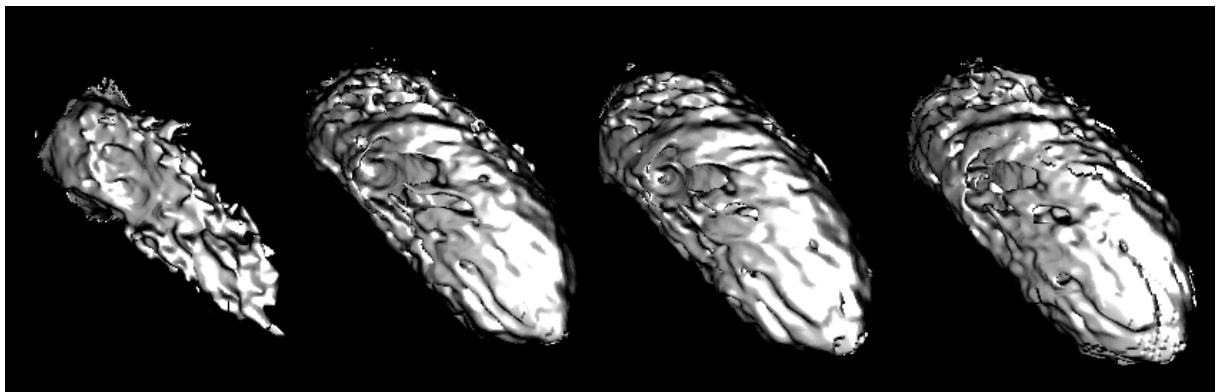


Figure 10. the left ventricle at different points in the cardiac cycle

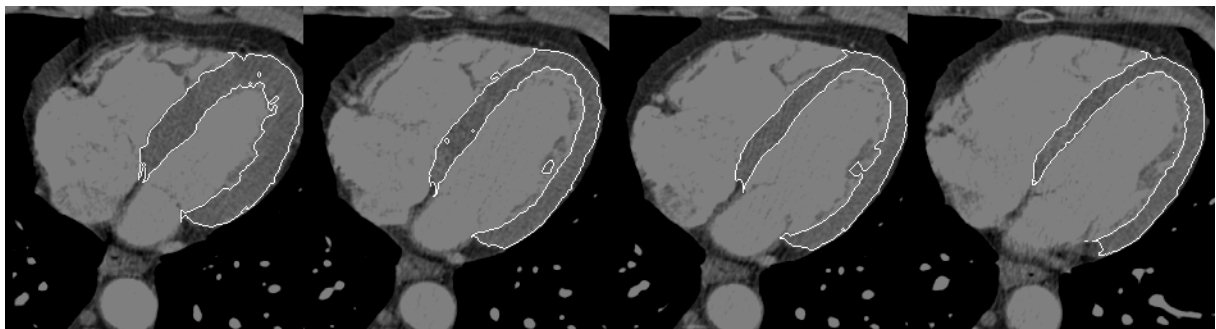


Figure 11. a cross section of the heart at different points in the cardiac cycle